RADAR BACKSCATTER MODELS OF POSSIBLE PYROCLASTIC DEPOSITS ON VENUS. I. Ganesh[1], L. M. Carter[1] and T.N. Henz[1], [1]Department of Planetary Sciences, University of Arizona. Tucson. Email: indujaa@email.arizona.edu.

Introduction: Radar-bright, diffuse deposits found on volcanic summits in Eistla Regio and Dione Regio have been interpreted as pyroclastic flow deposits [1-4]. They exhibit high backscatter and high RMS slopes in the 12.6 cm Magellan radar data, and high circular polarization ratio (CPR) in the Arecibo Observatory radar data; this has been interpreted to be caused by centimeter-scale surface roughness and centimeter-sized clasts [4]. Specific knowledge of properties like surface roughness and grain size distribution (GSD) is important for gaining insight into the formation, emplacement, and physical properties of the proposed pyroclastic deposits. Here, we attempt to place more quantitative bounds on these parameters through radar scattering and emission models of theoretical deposits.

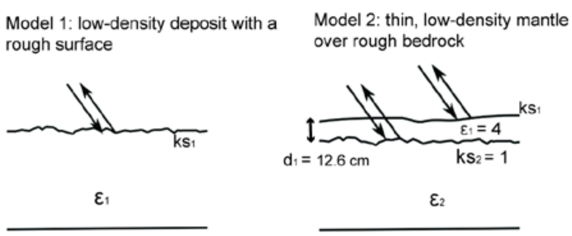

Figure 1: Schematic representations of the two pyroclastic deposit structures modeled.

Data and Methods: We consider different 1- and 2- layer pyroclastic models that could generate high backscatter and CPR (see Figure 1 for examples). We use the improved integral equation method (I^2EM) to compute scattering from surface and subsurface interfaces, and a vector radiative transfer approach for scattering from volumetric inclusions [5-7]. Our initial analyses are focused on pyroclastic models without any internal scatterers. Scattering results from two such models — 1) thick, low-density deposit with a rough surface, and 2) thin low-density deposit on top of a rough substrate (see Figure 1) — are presented here. Input parameters varied include layer thickness (d_1), dielectric permittivity of both layers ($\varepsilon_1, \varepsilon_2$), surface ($ks_1$) and subsurface ($ks_2$) roughness. The backscatter in HH polarization (σ_{HH}) computed is compared with Magellan backscatter coefficient of deposits at the summit of Irnini and Anala Mons [8].

Preliminary results: Figures 2A and 2B show the total backscatter in HH from models 1 and 2, respectively. The shaded grey area marks the range of backscatter values measured from Magellan datasets. In Figure 2A, the steep portion of the curve for $ks_1 < 1$ denotes an increase in backscattered radiation with increasing surface roughness at sub-wavelength scales. The surface appears roughest to the radar between ks_1 = 1 and ks_1 = 1.5–1.8. In this region, the measured values of Magellan radar backscatter are well-matched by model permittivity values between ε_1 = 4 and ε_1 = 7. For surface height fluctuations larger than the wavelength (ks_1 > 2), there is reduced backscattering and more coherent scattering. In Figure 2B, an increase in total backscatter with increasing ε'_2 is noticeable when the upper surface roughness $ks_1 \leq 0.5$. For larger values of ks_1 (> 0.5), the backscatter is independent of substrate permittivity, indicating that the total return is dominated by scattering from the upper surface of the mantling deposit.

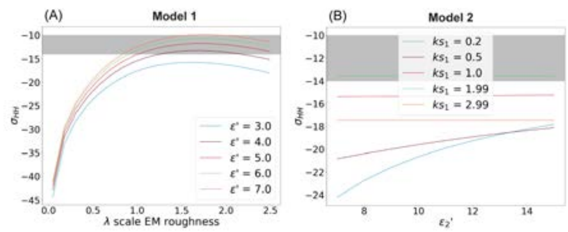

Figure 2: Backscatter σ_{HH} corresponding to (A) model 1 and (B) model 2.

Discussion: Results show that large radar backscatter returns that match Magellan observations need significant surface roughness at wavelength scale. A low-density deposit (ε'_1 = 4 to 6) without internal scatterers, similar to a lithic-poor ash flow deposit, having an electromagnetic surface roughness of ks_1 = 1–1.8 would conform to the radar observations. Subsurface backscatter from buried interfaces is dominant only when the surface layer has low reflectivity ($\varepsilon'_1 \leq 4$) and low surface roughness ($ks_1 \leq$ 0.5). Even then, the total backscatter is insufficient to produce the values seen in Magellan data.

Future work: Ongoing and future investigations include 1) testing more pyroclastic models that incorporate volume scattering, and 2) using Arecibo polarimetry measurements to place further constraints in order to develop a more comprehensive insight into the physical properties of these deposits.

References: [1] McGill, G. E. (2000). *USGS Sci. Inv. Map* 2637.[2] Campbell, B. A. and Clark, D. A. (2006), *USGS Sci. Inv. Map 2897*. [3] Keddie S. T. and Head, J. W. (1995) *JGR*, *100*, 11729-11753. [4] Campbell B. A. et al. (2017) *JGR*, *122*, 1580–1596. [5] Fung A.K. et al. (2002), *J. Electromagn. Waves Appl.*, *16*, 689-702. [6] Tsang, L. et al. (1985), *Theory of Microwave Remote Sensing*. [7] Fa et al. (2011), *JGR*, *116*, E03005. [8] Henz, T. N. et al. (2021*) 52nd LPSC*, Abstract #2150.